Percolation of a simulated metallic film on a porous substrate: The copper-polyimide interface

B. D. Silverman and D. E. Platt
IBM Research Division, Thomas J. Watson Research Center, Yorktown Heights, New York 10598
(Received 11 November 1992)

A simulation of the copper-polyimide interface previously investigated at low coverage is extended into the regime of higher metal-atom coverages. The evolution of film growth spanning regimes of independent cluster formation, percolating cluster formation, and continuous pinhole-free film growth is examined within the context of the model. Characterization of the "fuzzy" interface formed by metallic deposition onto a porous substrate is discussed. The effect of attractive metallic interactions and consequent induced-particle correlations on the percolation threshold of the deposit is examined. Enhancement or suppression of this threshold is found to depend upon the defined range of connectivity. Finite-size scaling in connection with the algorithm simulating deposition onto a cold substrate has been examined. Critical indices of the thin-film correlation length obtained for this three-dimensional simulation model with significant concentration gradient have been found to exhibit two-dimensional universal behavior within the accuracy of the calculations. The dependence of the percolation transition on the lattice anisotropy and interaction anisotropy is described.

PACS number(s): 05.50.+q, 64.60.Cn, 68.35.Rh, 68.55.Jk

I. INTRODUCTION

The deposition of metal atoms onto a porous polymeric substrate has been previously simulated [1] in connection with the interpretation of experimentally observed copper-atom diffusion into a polyimide substrate. Since the experimental studies [2] had been performed at low metal-atom coverages, namely, at approximately one-quarter monolayer coverages, the simulation model initially addressed issues relevant to the incipient stages of film formation. The purpose of the present paper is to describe the results obtained for the simulation model in the regime of higher metal-atom coverage. Issues that arise as a consequence of these investigations make contact with numerous other studies of simple models used to simulate the processes of deposition, diffusion, aggregation, and percolation associated with thin-film interfacial growth phenomena. One intriguing aspect of the present model is that it provides one with the ability to investigate details associated with any or all of these processes concurrently, i.e., with use of one single model.

The initiation of percolation of a metallic deposit on a disordered substrate is one interesting and important step in the evolution to continuous thin-film growth. Different aspects of such percolation have been the subject of extensive discussion. Two-dimensional micrographs have suggested the validity of universal scaling in the vicinity of the percolation threshold [3,4]. The role of particle connectedness and interaction-induced particle correlations have also been investigated in connection with the enhancement or suppression of the percolation threshold [5–8]. The significance and effect of a concentration gradient on the percolation threshold have also been examined [9].

Bug *et al.* [5] examined an interactive percolation model in two and three dimensions. They showed that the percolation concentration depended upon the interaction volume, the interaction depth, and the connectivity length. In particular, they showed that depending on the connectivity length, the percolation concentration would increase or decrease. DeSimone, Stratt, and Demoulini [8] examined a similar question from the standpoint of the Percus-Yevick equation, namely, by examining percolation in a liquid. Albano and Martin [7] showed that for deposition onto a two-dimensional substrate, the percolation concentration decreased with increasing interaction energy. This result was consistent with the shorter connectivity regime investigated by Bug *et al.* [5]. By simulations in two and three dimensions, Hayward, Heerman, and Binder [6] had also shown that the percolation concentration was lowered by interactions. They also explored the universality class of percolation in the presence of interactions.

The practical problem of modeling the deposition of copper onto a polyimide substrate is of importance in the design of electronic devices as well as in understanding some of the physics of failure in devices constructed at smaller and smaller length scales. In the real world, copper as deposited onto the polymer yields a $(2+1)$-dimensional deposition problem. The present paper, therefore, investigates a model that is more general than treated in the previously referenced work. The present model, previously described by Silverman [1], examines the deposition of copper onto a polyimide substrate with use of a two-component Ising model on a lattice. It treats the problem as a $(2+1)$-dimensional deposition-percolation problem. In this context we see percolation paths that are completed in two dimensions, but which have connectivity through the third dimension in the layers of copper that have been deposited on the surface of

the polyimide. The polyimide also diffuses, being self-repulsive as well as exhibiting attraction to the copper. The copper atoms are attracted strongly to themselves and weakly to the polyimide. From the perspective of modeling copper deposition, the lattice is introduced as an approximation. The behavior of the percolation threshold as a function of lattice-induced parameters, such as connectivity length, coordination number, lattice-induced anisotropy, and interaction range, therefore requires careful treatment in the context of understanding percolation in a $(2+1)$-dimensional deposition. Another feature of interest in this $(2+1)$-dimensional system is the impact on the universality of the critical indices of percolation due to connectivity through the third dimension. The present simulation clearly highlights features that are partly two dimensional and partly three dimensional and raises a number of interesting issues concerning universality. The subject of percolation in a concentration gradient involving Fickian diffusion has been previously studied by Kolb *et al.* [9].

In the present paper we will examine several percolative characteristics of the three-dimensional simulation model. First, the critical concentration p_c of the deposited film will be determined for two different definitions of connectivity. The first, when nearest-neighbor metal atoms on the three-dimensional grid determine connectivity, will be referred to as the case of "near" connectivity. The second, when nearest as well as next-nearest-neighbor metal atoms are considered to be connected, will be referred to as the case of "far" connectivity. It will be shown that the critical indices obtained for scaling of the two different percolating cluster correlation lengths are similar and scale with values near the two-dimensional value. Since the metal-atom deposit exhibits a relatively rapid decay in concentration in the direction normal to the film surface, percolation when it occurs involves connected paths that are essentially transverse to this normal.

It will be shown upon annealing that attractive interactions enhance percolation for the case of near connectivity, while they suppress percolation for the case of far connectivity. The suppression is a simple consequence of the low density of material required for percolation involving far connectivity and the consequent clustering induced by attractive interactions. The enhancement involving near connectivity is a consequence of induced correlations possible at higher concentrations. Furthermore, it will be pointed out that annealing introduces a length scale that is large compared with either of the near or far connectivity lengths and, consequently, the percolation threshold involving the two different definitions of connectivity becomes comparable after annealing.

Several other interesting questions arise within the context of the three-dimensional model. For example, what is the nature of the "fuzzy" interface obtained at the higher coverages and how might such an interface be conveniently described? What is the distribution of "screened" clusters beneath the continuously evolving connected film above? Furthermore, what are the statistics associated with creating pinhole-free films at higher metal-atom coverages and what are the factors that either enhance or suppress the creation of such pinhole-free continuous films?

II. MODEL

The deposition model and results in the low-deposition regime have been previously described [1]. We will review details of the deposition model in the present section. Various components of the model had been included not only to simulate processes observed during the radio tracer diffusion studies [2] at low metal-atom coverages, but to also simulate certain observed features in TEM micrographs obtained at higher metal-atom coverages [10,11]. The potential parameter space that one might investigate in connection with the model is vast, and as a consequence the present as well as the previous study [1] have examined an exceedingly narrow range of this space. The model includes mechanisms for simulating the following practical experimental effects. Annealing of the metal-polymer interface has played a major role in the experimental studies and therefore temperature has been included in the simulation via a Monte Carlo procedure. The choice of interaction energies places the simulation model in an extreme island growth regime. Thermally activated single-particle Fickian diffusion has been experimentally observed [2,11] at significant distances from the interface. The observed temperature dependence of this single-particle Fickian diffusion has provided a connection between the thermally activated Brownian motion of the simulation model and experiment. As a consequence, the metal-atom-polymer interaction energy has been chosen to be significantly weaker than the interaction energies between metal atoms. It is this relatively weak binding between metal atoms and the polyimide which is responsible for the poor adhesion of copper films to this polymer substrate.

The model is defined by the following idealizations and processes. The polymer has been idealized by a set of interaction sites. In a sense, the polyimides are structurally intermediate to polymers, such as polyethylene, which exhibit a significant degree of backbone torsional freedom and molecular crystals composed of stacked aromatic units. Films of these materials are known to be composed of local regions exhibiting varying degrees of crystalline order [12,13]. Variation of the interaction energies chosen between the set of polymer interaction sites allows the simulation of varying degrees of polymeric structural order. The interaction sites are chosen to be mobile since micrographs [10] suggest that metal-atom cluster formation within the polymer is accompanied by the extrusion of polymeric material. The polymeric interaction sites are distributed on a three-dimensional grid and metal-atom migration is only allowed onto sites that are not occupied by either a polymeric interaction site or another metal atom. The density of interaction sites chosen therefore determines the space available for metal-atom migration. This density has been initially chosen so that simulated single-particle diffusion into the polymer corresponds qualitatively with that observed by the radio tracer diffusion studies [2].

An interesting range of parameters not yet investigated in detail involves the ratio of the average metal-atom

deposition rate to the metal-atom migration rate. One expects a significant variation in the metal-polymer interfacial structure as a function of this ratio. As expected, rapid deposition with respect to migration yields the more clearly defined interface in the experiment [10] as well as in the simulation. In the present paper we have assumed that all depositions are rapid compared with migration rates and therefore all subsequent migration due to annealing arises from a metallic layer already present at the surface or interface.

One independent variable of a spatially uniform percolation theory is the site-bond occupation probability [14]. In the present simulation, the spatially nonuniform average site occupation probability is a strongly varying function of the total amount of material deposited, as well as being dependent upon other model parameters determining deposition, diffusion, and aggregation. A convenient independent variable of the present simulation is, therefore, the total amount of material (number of metal atoms or monolayers) deposited. This, together with the lattice size of the simulation volume, can be treated as independent variables of the simulation, in much the same manner that they are treated in finite-size scaling treatments of ballistic aggregation models [15,16].

Percolation in a concentration gradient has been previously discussed in connection with a metal-polyimide interface [9,17]. The metal-atom distribution at the interface was generated by simulating statistics associated with Fickian diffusion from a continuous metal-atom source. The results of the simulation were discussed in connection with experiments involving the process of electrodeposition of continuous silver metal films at a polyimide-cathode interface [18]. The calculations described in the present paper have attempted to simulate thermal evaporation of metal atoms onto a clean polyimide surface in an ultrahigh vacuum. Consequently, metal-atom clustering at the interface and subsequent aggregation and growth processes in the evolution to continuous-film growth have been of central interest.

The model uses a Metropolis algorithm to simulate diffusive and bonding processes. This implies that the true Hamiltonian, which would include kinetic energy and potential energy, has been effectively integrated out to produce this simpler form. The diffusion process is modeled by the transition rules of the Metropolis algorithm. This implies that connections to real experiments must be made through lumped parameters such as the step size. The step size defines the mobility distribution of this model. The mobility distribution defines the effective cluster sizes, forming the connection between the model length scale and observed colloidal cluster sizes.

III. FUZZY INTERFACE

Metallic deposition onto a porous substrate spans several interesting regimes of growth. Initially, at low deposition, clusters form at the surface as well as in the interior of the film. As these clusters grow in size upon increasing deposition, they reach sizes at which they begin to coalesce. Concurrent growth and coalescence ultimately yield a connected, percolating structure which can be identified as the incipient "thin film." In the vicinity of the percolation threshold, the distribution of disconnected screened clusters beneath the film-substrate interface approaches a steady state that is essentially independent of further deposition as the thin film above the interface grows in size proportional to the amount of deposited material. Further deposition ultimately yields a continuous, pinhole-free, thin film.

The present section will illustrate these different regimes of growth by modeling deposition onto a cold substrate, i.e., where thermal migration of the metal-atom deposit is inhibited. It should be emphasized that many of the phenomena investigated are nonuniversal, depending in detail upon the deposition conditions. On the other hand, the next section will examine results of finite-size scaling in the vicinity of the percolation threshold. Finite-size scaling indicates that the critical exponents of the cluster correlation lengths for the two different connectivity definitions exhibit universal behavior.

Initially, as deposition begins, there is an overall growth in cluster size. The previous investigation [1] examined the distribution of cluster size at one-quarter monolayer deposition, i.e., within a deposition regime well below the percolation threshold for either of the types of connectivity, near or far. At such lower deposition all clusters are relatively small. As deposition proceeds and one connected percolating cluster emerges, the distribution of screened, disconnected clusters becomes stationary and spans a relatively small range of cluster sizes. The small range of cluster sizes of the disconnected cluster distribution is a consequence of the sharp concentration gradient. Characteristics of this screened distribution will be examined subsequently.

Figure 1 is a plot of the largest cluster size as a function of the number of monolayers deposited. For the 81×81 transverse dimensions of the model, one monolayer is equivalent to 6561 deposited metal atoms. Cluster size in the figure is given as the number of metal atoms in the cluster. For this figure, as well as for this entire section, it will be assumed that percolation is defined in terms of far connectivity. Furthermore, all figures in this section have been obtained by taking averages over five different depositions unless otherwise noted. Initially, at low deposition, one sees a rapid increase in cluster size as a function of deposition. This is the regime where cluster growth is controlled by the capture of deposited material as well as by the coalescence of adjacent clusters. Just above the percolation threshold (shown by the vertical dashed line) of the growing film, one sees the onset of the regime where most of the deposited metal atoms are captured by the connected film and the growth of the major cluster or connected film proceeds linearly with the amount of material deposited.

Figure 2 is a plot of disconnected cluster number as a function of the amount of material deposited. The disconnected cluster number has been defined as the difference between the total number of clusters and the largest cluster. While such a definition is not particularly meaningful in the low-deposition regime, in the limit of large deposition it is just the number of disconnected clusters beneath the growing film. At low deposition this

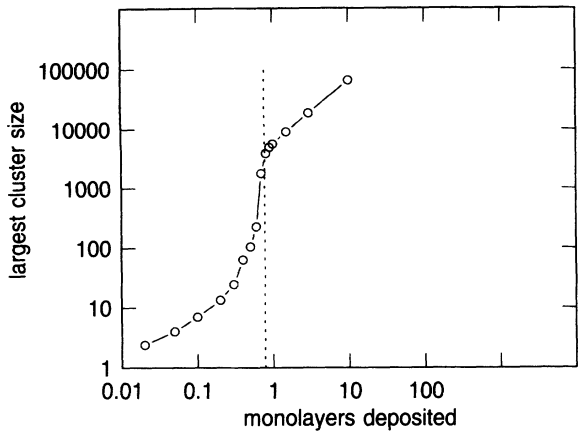

FIG. 1. Size of the largest cluster as a function of the number of monolayers deposited. The dashed line is at the value for which 90% of the depositions yield at least one percolating structure for the $81\times81\times51$ simulation volume.

number grows rapidly with the amount of material deposited. At approximately 0.1 monolayer below the percolation threshold the curve abruptly turns around, reflecting the rapid onset at which adjacent clusters begin to coalesce and create the connected percolating film. The distribution of disconnected clusters then plunges until it becomes independent of deposition and is just the screened number of clusters below the film-substrate interface.

How might one quantitatively characterize such a fuzzy interface at the onset of formation of a connected percolating film as well into the regime of higher deposition? One might define this interface as consisting of the boundary that separates the percolating film from the substrate as well as the distribution of independent clusters beneath such a boundary. The boundary can furthermore be characterized in several different ways. In a manner analogous to a description of the active growth zone of deposition models [15,19], one can calculate the mean depth and width of the interface between the substrate and the connected percolating film. The mean interfacial depths of the film is calculated by averaging the greatest penetration of the film into the substrate at index k of the film over all i,j's. The root-mean-square variation about this mean depth can then be calculated. Furthermore, a lower hull [20,21] or "bottom" surface perimeter of the percolating film on the substrate may be defined by including only that portion that penetrates into the region where the substrate exists. For the present model, it has been previously pointed out [1] that one may consider the polymer surface to be at $k=-20$ even though no interaction sites are present locally at this value of index.

Figure 3(a) illustrates the penetration profile into the substrate of a percolating cluster consisting of 2660 metal atoms. This is given as a function of the index k. This particular connected cluster was formed during one-monolayer deposition (6561 metal atoms). The profile, a

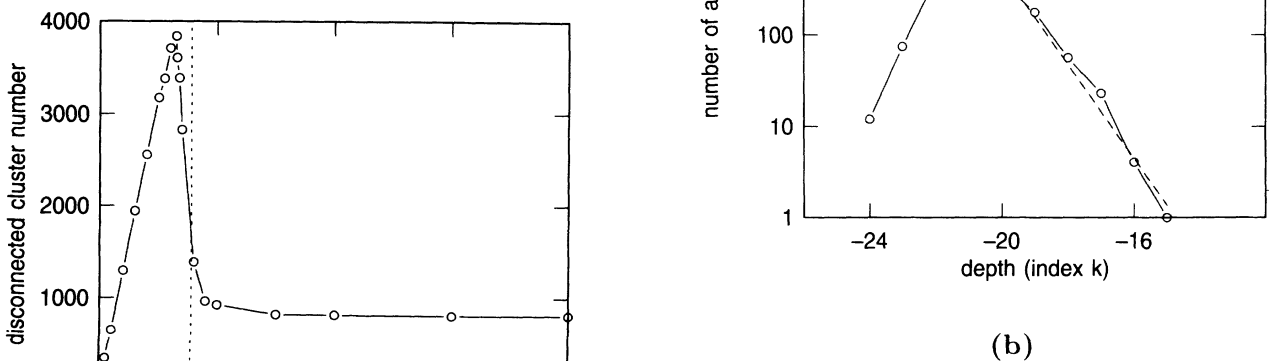

FIG. 2. Disconnected cluster number as a function of the number of monolayers deposited. Dashed line defined as in Fig. 1.

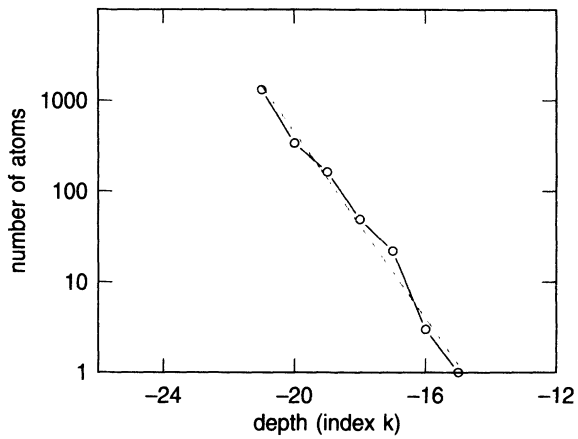

(a)

(b)

FIG. 3. (a) Number of atoms at maximum penetration into the substrate for a percolating film consisting of 2660 metal atoms. Slope of the least-squares-fitted line shown is -0.511 ± 0.027. (b) Number of atoms at each depth of the 2660-metal-atom film for which calculations in (a) are exhibited. Slope of the least-squares-fitted line shown is -0.514 ± 0.025.

measure of interfacial penetration, was obtained by summing the number of metal atoms belonging to the percolating cluster at a given k that are at maximum depth for each i,j. This is just the distribution of metal atoms at the film-substrate interface used to calculate the mean depth of interfacial penetration. Figure 3(b) is a similar plot to 3(a) but we have now counted all of the 2660 metal atoms in the cluster. Values of metal-atom positions for which $k < -20$ give the distribution of metal atoms that are above what we have previously defined [1] to be the film surface.

In Fig. 4 we have plotted the mean film depth of the interface as a function of monolayer coverage. Again, averages over five different depositions have been used. From the values shown in this figure, and the distribution shown in Fig. 3, one surmises that the deposition algorithm yields little penetration of the percolating film into the substrate since the mean depth is intermediate to the substrate layer at $k = -20$ and the layer just above at $k = -21$. Examination of the figure shows the increase and onset of saturation of mean depth as an increasing amount of material is deposited.

Figure 5 shows a slice, perpendicular to one of the transverse directions of the film-substrate interface, for a deposit of three monolayers. This figure reveals the two-dimensional character of the film being formed as well as metal-atom penetration beneath the film.

Figures 6(a) and 6(b) are semilogarithmic and log plots of the number of disconnected clusters as a function of cluster size for four monolayers of deposition. At such enhanced deposition, the disconnected number of clusters with increasing deposition has been saturated. Examination of these two figures shows the distribution to be, over the range of smaller cluster size, intermediate to exponential and power-law behavior. The development of a detailed understanding of the origin of such a distribution of small clusters in a nonuniform concentration gradient might utilize concepts involved in the examination of the distribution of lattice animals of a spatially uniform percolation theory [14]. It is of interest that such lattice animal distributions also exhibit behavior that is intermediate to an exponential and power law [22].

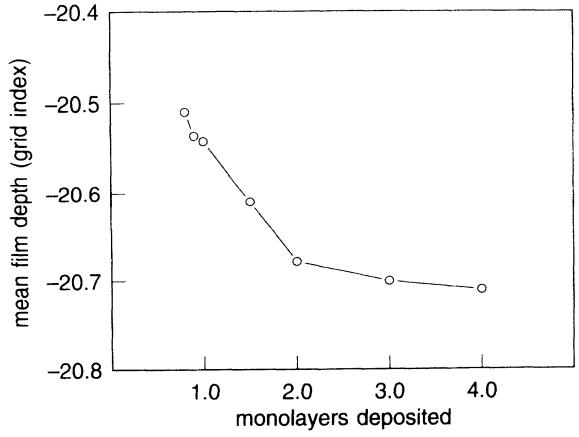

FIG. 4. Mean film depth as a function of the number of monolayers deposited.

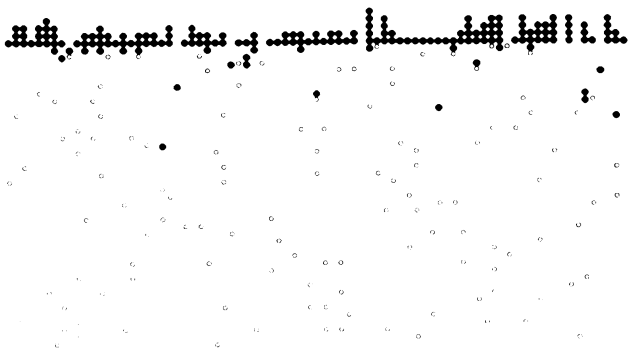

FIG. 5. A slice, perpendicular to one of the transverse directions, of the film-substrate interface for a deposit of three monolayers.

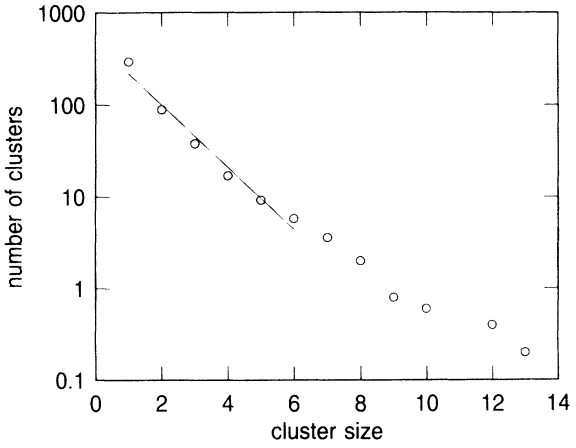

(a)

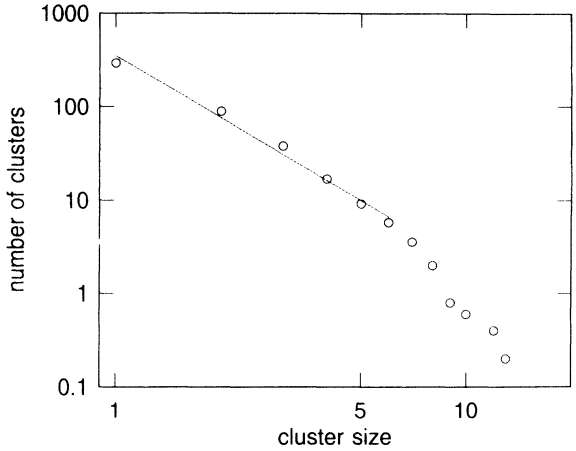

(b)

FIG. 6. (a) Semilogarithmic plot of number of clusters as a function of cluster size. Slope of the least-squares-fitted line shown is -0.338 ± 0.026. Over the range of small cluster sizes the decrease with increasing cluster size is seen to be less rapid than an exponential. (b) Log plot of number of clusters as a function of cluster size. Slope of the least-squares-fitted line shown is -2.21 ± 0.12. Over the range of small cluster sizes the decrease with increasing cluster size is seen to be more rapid than a power law.

While the percolation regime of film growth is of interest, not only in connection with a number of formal questions relating to percolation theory, but also in connection with a number of practical issues, e.g., the minimal amount of material required to form a conducting film, this film growth regime is not the only one of practical interest. The objective of most film synthesis is to create pinhole-free continuous films. We have, therefore, been motivated to extend the simulations into a regime of higher deposition and to consider what might be meant by a pinhole-free film within the context of the present model. For simplicity, we have defined a pinhole as any "open" or metal-free vertical channel extending through the percolating film. Formally, this means that for any fixed i and j, there exists no value of the index k such that the position i,j,k has a metal atom present that belongs to the percolating cluster. If this condition holds, then we say that there is a pinhole in the connected film at the lateral location i,j. This definition will suffice for the quasi-two-dimensional films generated by our deposition algorithm. A more highly crenellated film texture will require a more general definition.

Figure 7 shows the calculated fraction of pinholes as a function of monolayer coverage. Again, we have averaged over five percolating structures at each different deposition. This fraction is just the ratio of open channels to the total number (6561) of channels. Figure 8 shows a top view of one of the percolating structures obtained at two monolayers of deposition. In this figure an empty site indicates the location of what we have defined as a pinhole. Open connected structures of a number of different sizes and shapes are apparent in the figure and are formed by different arrangements of adjacent single empty channels. It should be emphasized that Fig. 8 is not a picture of metal-atom coverages in a channel arising from the total distribution of metal atoms deposited. Such metal-atom coverage on average is simply given by $P=1-\exp(-m)$, with P the probability that at least one metal atom is in the channel and m the number of monolayers deposited. On the other hand, the percentage of open channels or pinholes in a percolating cluster for any given amount of material deposited will be a strong function of the average penetration depth determined by the deposition algorithm.

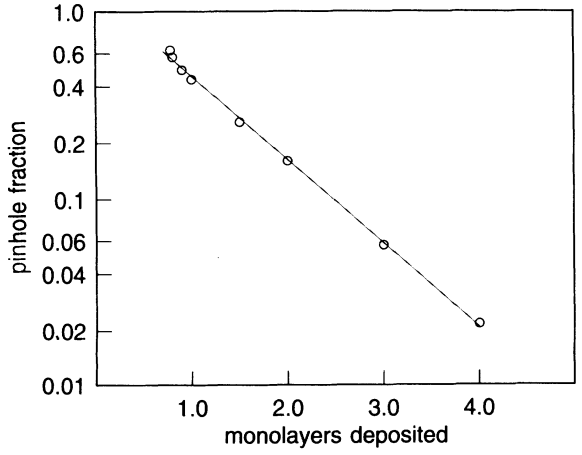

FIG. 7. Pinhole fraction as a function of monolayer coverage. Slope of the least-squares-fitted line shown is -0.445 ± 0.0074.

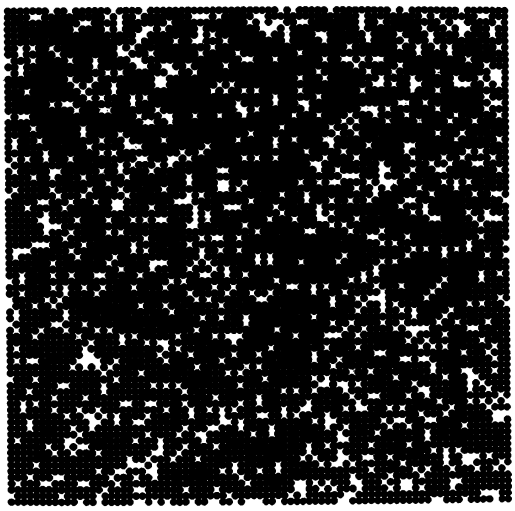

FIG. 8. Top view of the pinhole distribution for a percolating film generated during the deposition of two monolayers of metal atoms.

IV. PERCOLATING FILM ON A COLD SUBSTRATE

Figures 9 and 10 show the fraction of depositions on a cold substrate as a function of monolayer coverage that yields percolating films. All connected paths found are transverse to the substrate surface due to the significant metal-atom concentration gradient perpendicular to this surface. Calculations were performed for five different square lattices with transverse widths of 16, 32, 64, 128, and 256 lattice spacings. The calculations described in this section have been particularly developed to address issues relevant to finite-size scaling and universality. Figures 9 and 10 illustrate results obtained for near and far connectivity, respectively. If it is assumed that only nearest-neighbor metal atoms are connected, i.e., near connectivity, then the fixed point p_c shown in Fig. 9 occurs at a value of deposition that is significantly greater than one monolayer. If far connectivity is assumed, percolation threshold values, as shown in Fig. 10, are shifted to values significantly below one monolayer. Several hundred runs have been averaged to obtain each of the value shown in the figures. The number of runs, ranging from 200 to 800, were chosen to be dependent upon the cpu time required to catalog the clusters and check for percolation. The shorter cpu time required for the cluster and percolation analysis, for near connectivity, provided the opportunity of performing a greater number of runs than for far connectivity, hence the greater number of data points shown in Fig. 9 than in Fig. 10.

The number of percolating depositions as a function of monolayer coverage has been fitted to a Gaussian sigmoid F to obtain the effective critical monolayer coverage p_c and the standard deviation for an infinite system. The transitions and standard deviations for each lattice size were used to construct the finite-size scaling behavior.

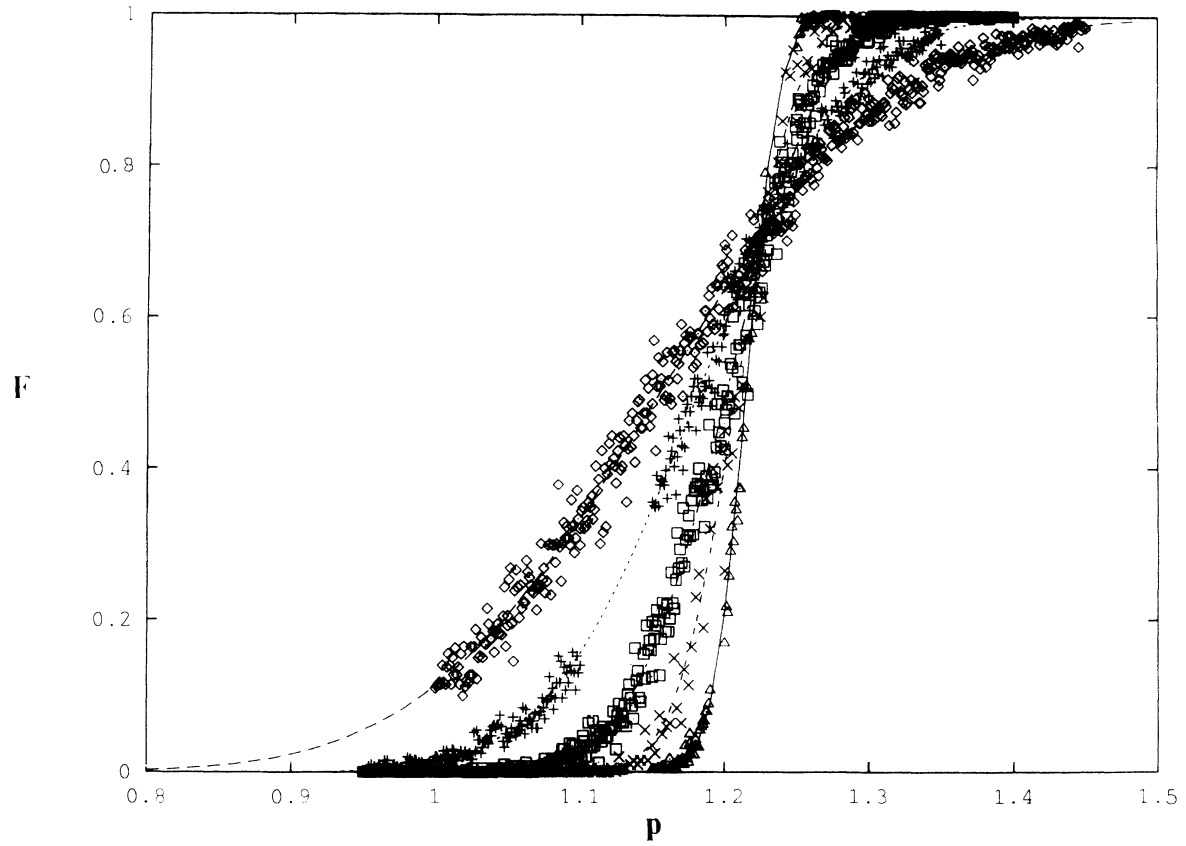

FIG. 9. Fraction of percolating depositions as a function of monolayer coverage for the definition of near connectivity. Diamonds for a lattice of transverse dimensions 16×16; pluses, 32×32; squares, 64×64; crosses, 128×128; triangles, 256×256.

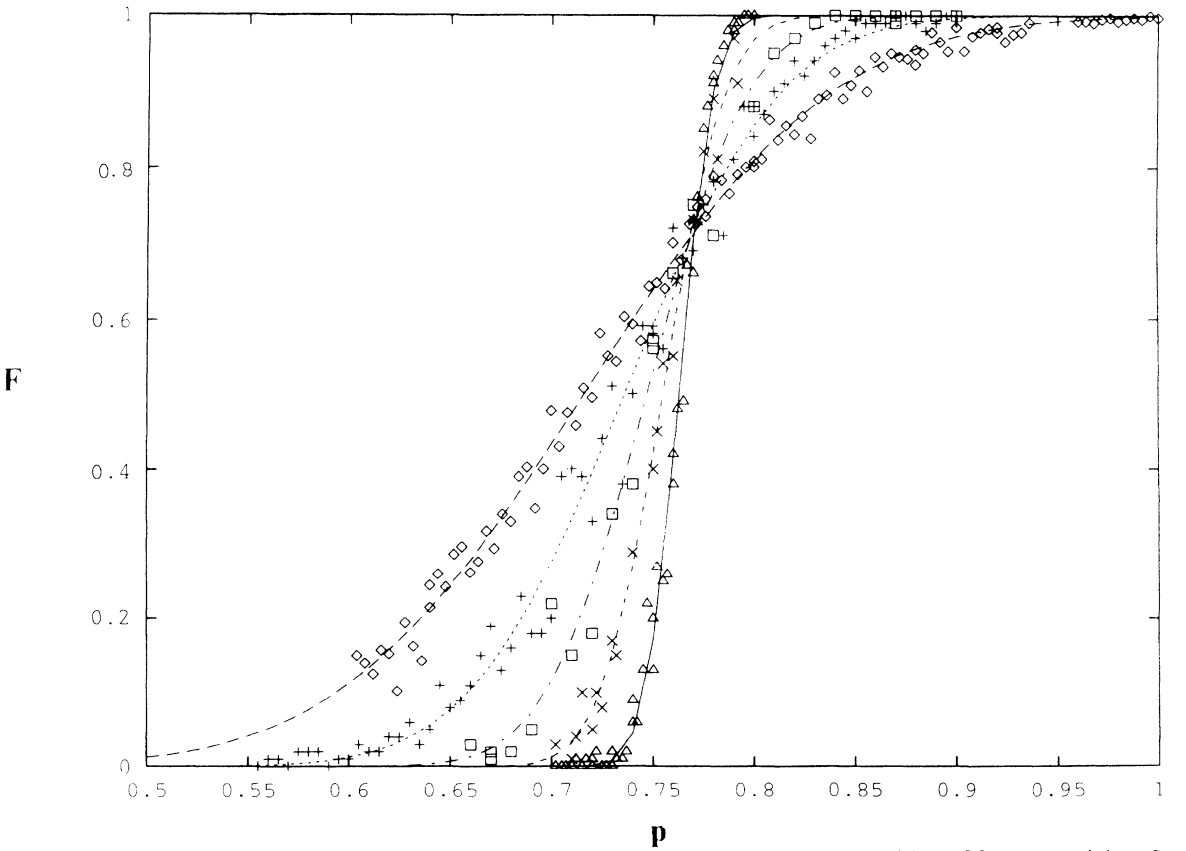

FIG. 10. Fraction of percolating depositions as a function of monolayer coverage for the definition of far connectivity. Symbols as defined in Fig. 9.

The function F fitted is

$$F(p;p_c(L),\sigma(L))=\frac{1}{\sqrt{2\pi\sigma^2(L)}}\times\int_{-\infty}^{p}dz\exp\left[\frac{-[z-p_c(L)]^2}{2\sigma^2(L)}\right] \tag{4.1}$$

or

$$F(p;p_c(L),\sigma(L))=\frac{1}{2}\left[1+\mathrm{erf}\left[\frac{p-p_c(L)}{\sqrt{2}\sigma(L)}\right]\right], \tag{4.2}$$

where

$$p_c(L)=p_c(\infty)-\alpha L^{-\gamma}, \tag{4.3}$$

$$\sigma(L)=bL^{-\gamma}, \tag{4.4}$$

$$\mathrm{erf}(z)=\frac{2}{\sqrt{\pi}}\int_0^z dt\exp(-t^2). \tag{4.5}$$

Values of the scaling exponents are given in Table I. These scaling exponents are of particular interest, since they establish the universality of the percolation process.

Figures 11 and 12 show scaling collapse of the percolation transition for the different size lattices. This is achieved by recognizing that the argument of the error function in Eq. (4.2) is scale invariant. The fraction of clusters $F(p;p_c(L),\sigma(L))$ that percolate is then plotted against $(p-p_c(L))/\sigma(L)$ in Figs. 11 and 12.

TABLE I. Finite-size scaling parameters.

L	$p_c(L)$	$\sigma(L)$
	Near interactions	
16	1.155 4047	0.128 6929
32	1.181 7766	0.081 0648
64	1.201 3457	0.051 3333
128	1.208 0391	0.032 8327
256	1.214 6088	0.018 2668
	$\sigma=0.900\,196L^{(-0.693722)}$	
	$p_c=1.225\,513-0.477\,910L^{(-0.693722)}$	
	Far interactions	
16	0.716 190	0.095 7757
32	0.736 405	0.060 8780
64	0.746 985	0.039 3372
128	0.754 810	0.024 2594
256	0.762 756	0.013 4605
	$\sigma=0.687\,501L^{(-0.698923)}$	
	$p_c=0.768\,322-0.364\,150L^{(-0.698923)}$	

Since the deposited film has a finite thickness perpendicular to the percolating transverse directions, and percolation involves paths in three dimensions, the question arose as to whether the universality of the scaling would

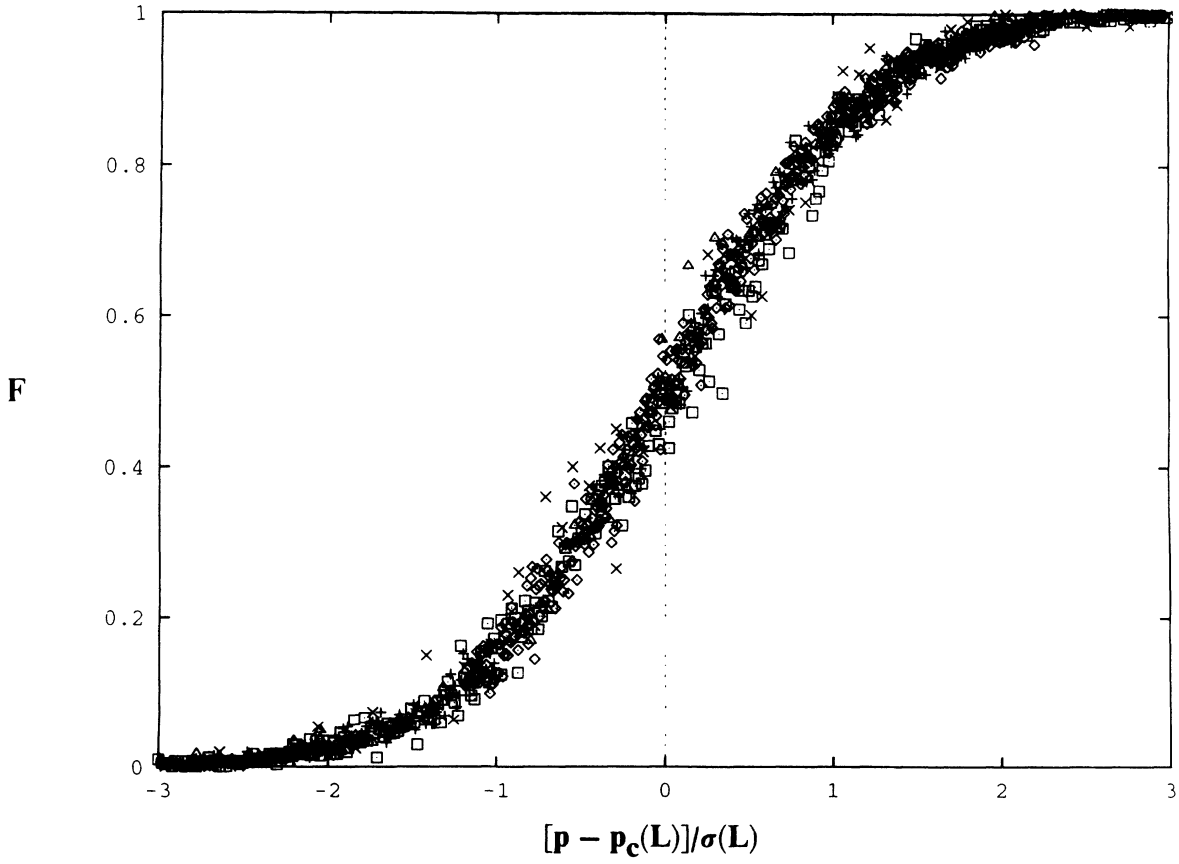

FIG. 11. Scale-invariant percolation probability as a function of the deviation of monolayer coverage from the fixed point for the definition of near connectivity.

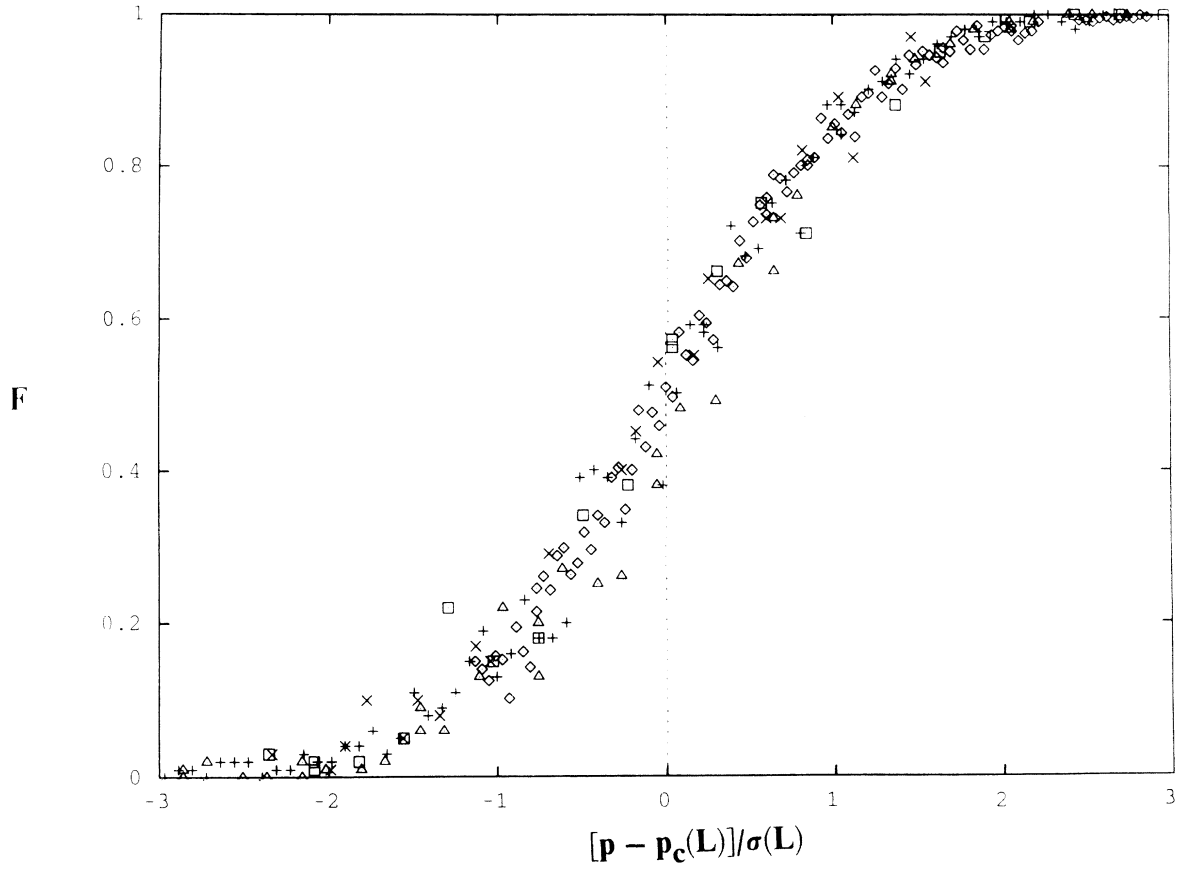

FIG. 12. Scale-invariant percolation probability as a function of the deviation of monolayer coverage from the fixed point for the definition of far connectivity.

be two dimensional or three dimensional. It was found (Table I), however, that the critical exponents of the correlation length of the infinite cluster, obtained for the two different definitions of connectivity, exhibit values that are close to the value obtained for two-dimensional percolation on a square lattice [14].

While the amount of deposited mass required to induce percolation is a sensitive function of the model parameters as well as the defined connectedness, it is also true that percolation, while it involves paths in three dimensions, occurs only in two dimensions. The deposition process is, therefore, treated as a $(2+1)$-dimensional problem, and the scaling of the lattice is only studied in two dimensions. Furthermore, as a consequence of the choice of model parameters, the depth of the deposit and the thickness of the cluster are small compared with the two-dimensional extent of the clusters. While the third dimension provides additional paths that would not have existed in two dimensions and consequently allows connections to occur that would otherwise not have occurred, the dominant universality obtained is still apparently two dimensional. Investigation of finite-size scaling in connection with a deposition algorithm that resulted in a broader penetration profile of metal atoms into the substrate with, however, a concentration gradient still sufficient to preclude percolation from occurring across the third dimension, yielded critical exponents that were also near the two-dimensional value. Apparently connectivity through the third dimension, with lattice periodicity imposed for that dimension, is required before one observes critical indices that deviate from the two-dimensional value.

V. ENHANCEMENT OR SUPPRESSION OF THE PERCOLATION THRESHOLD: ATTRACTIVE INTERACTIONS

The initial film morphology changes significantly upon annealing at an elevated temperature. Figure 13 is a top view of a 0.72-monolayer deposition prior to annealing. Different clusters are indicated by the different grey scales. Figure 14 shows a 1.1-monolayer deposition annealed at 320 °C [1]. The diffusion of metal atoms and consequent clustering is determined by the interactions between all constituents of the model system, the available free volume for diffusion, as well as by the cluster mobilities. The model resembles a multicomponent Ising model with the statistics for each transfer governed by the Metropolis algorithm. We have assumed transitions to occur by only single-particle nearest-neighbor jumps.

During annealing both polyimide interaction sites and copper atoms diffuse. Due to the relatively strong attractive interactions between copper atoms, polymeric interaction sites are generally extruded from the metal-atom clusters as they are formed. The quasi-steady-state cluster size is determined essentially by the sweeping up

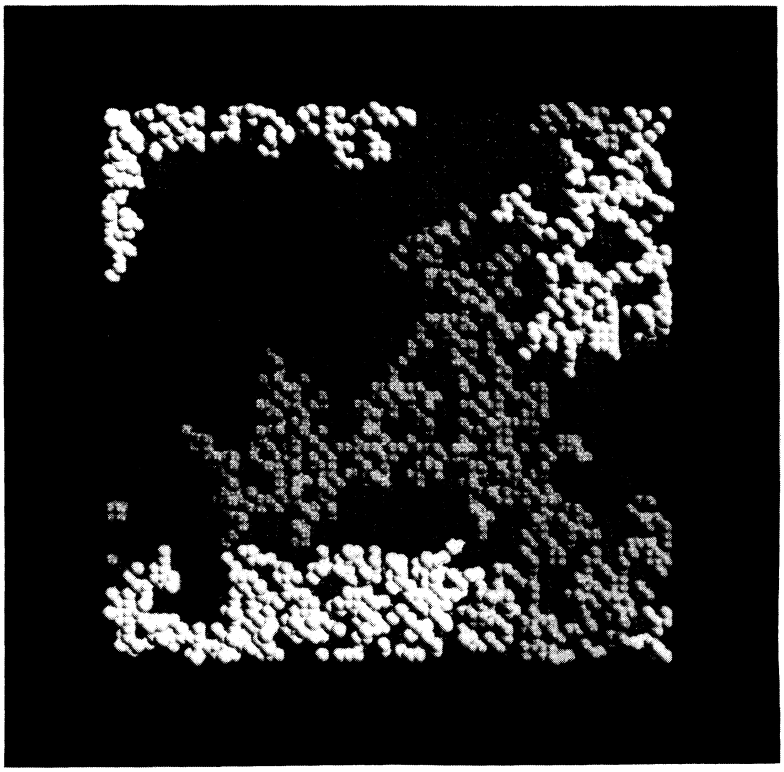

FIG. 13. Top view of a 0.72-monolayer deposition prior to annealing. Different grey scales indicate different clusters for far connectivity definition.

of the mobile single-metal atoms. At low deposition the clusters are compact or partially ramified, dependent upon details of the metal-atom interaction [1]. At higher deposition, the clusters coalesce to form "sausages" (Fig. 14). This is consistent with what had been found previously for an Ising system with attractive interactions just below the percolation threshold, namely, that the shape of the clusters near the critical percolation concentration is such that the mean boundary is proportional to the mean bulk [23]. Cluster sausage shapes have also been observed for gold films on an amorphous substrate [3].

Cluster distribution and percolation analyses have been performed for "weak" as well as "strong" metal-atom interactions subject to the two different connectivity

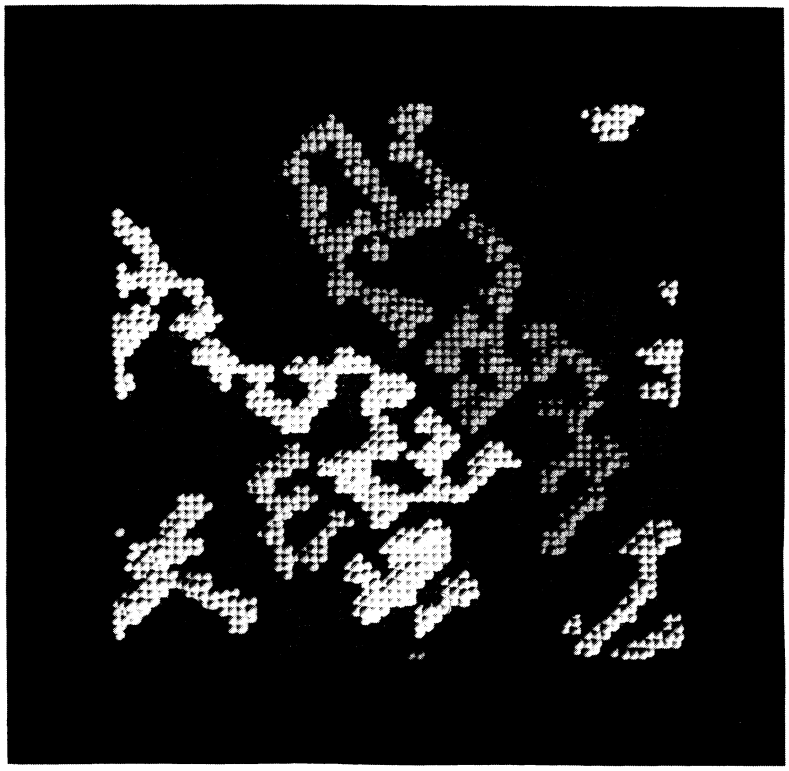

FIG. 14. Top view of a 1.1-monolayer deposition annealed at 320 °C. Different grey scales indicate different clusters for far connectivity definition. The metal-atom interaction is strong. Tiny spheres represent polymer interaction sites.

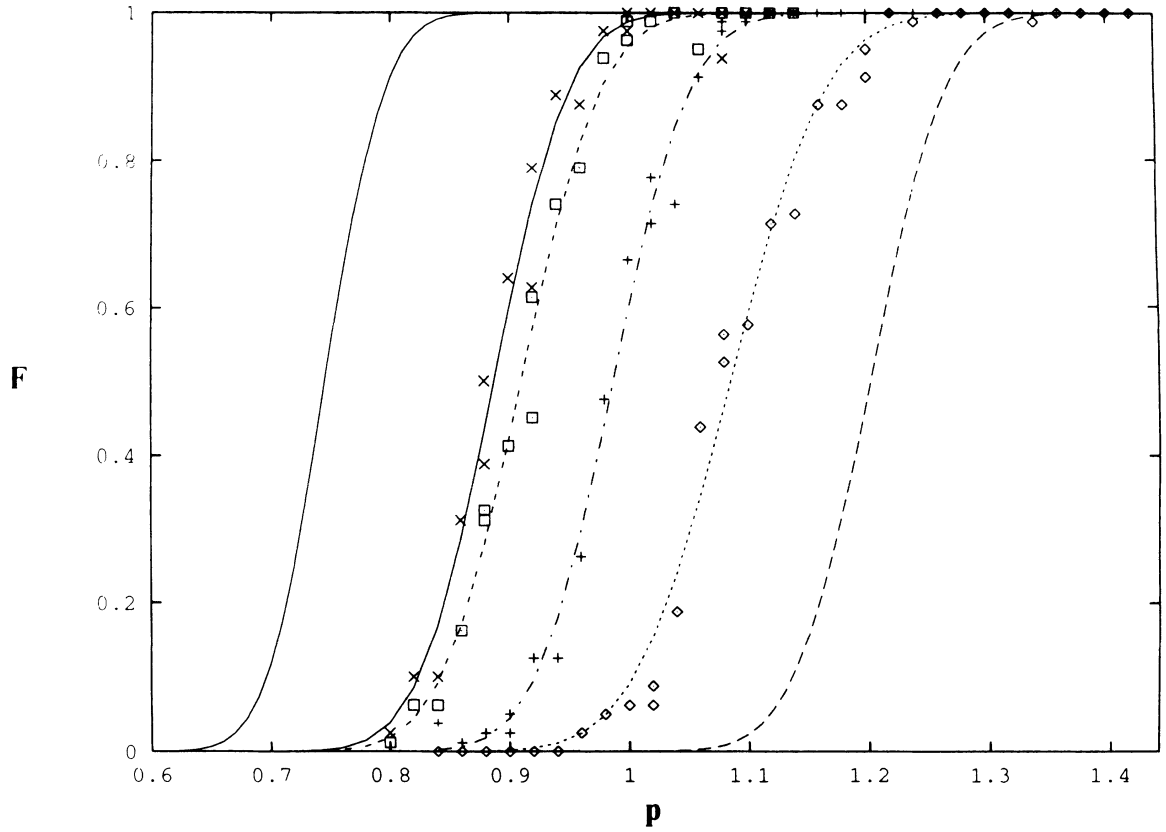

FIG. 15. Fraction of annealed percolating depositions as a function of monolayer coverage. Solid line, far connectivity unannealed; dashed line, near connectivity unannealed; cross and solid line: weak far; square and dashed line, weak near; plus and dashed-dotted line, strong far; diamond and dotted line, strong near.

definitions, near and far. Figure 15 shows percent percolation as a function of coverage for the different interaction strength and connectivity definitions. In the figure we have also plotted the results obtained for the two different connectivity definitions prior to annealing. The results obtained prior to annealing are shown without data points and exhibit percolation thresholds at the smallest and largest values of coverage p. All values given in Fig. 15 have been obtained for the model with transverse dimensions 64×64. Examining the figure one first notes that the percolation thresholds for all of the annealed systems investigated are closer to each other in coverage than for the systems with different connectivity definitions prior to annealing. Furthermore, one notes that for weak interaction, both curves for the two different connectivity definitions almost fall on top of each other. The proximity of the curves for the different connectivity definitions presumably occurs since the characteristic sausage thickness provides a length scale large compared with the distances between either nearest-neighbor lattice sites or next-nearest-neighbor lattice sites, consequently the near and far connectivity cluster maps are almost identical to each other.

It should be noted that for near connectivity, percolation now requires a smaller amount of deposited material than for the unannealed film. Such results had originally been obtained in a number of simulations involving attractive interactions. Far connectivity, on the other hand, yields contrasting behavior. More material is now required to enhance percolation than for the unannealed film. The suppression of the percolation threshold after annealing is apparently a consequence of the low density of material required for percolation involving far connectivity prior to annealing and the consequent clustering induced after annealing. The enhancement upon annealing of the system connected by only nearest-neighbor metal atoms is a consequence of induced correlations at the higher concentrations involving structures that are degenerate in energy with the less correlated structures of the unannealed system.

Upon annealing, the behavior of the strongly interacting systems for the two different connectivity definitions is similar; however, the two curves are not in the same close proximity as found for the weakly interacting systems. This distinction between the behavior of strongly and weakly interacting systems might result from the enhanced diagonal connections induced in the strongly interacting system and the connectivity definition which distinguishes such connections. Diagonal connections are not energetically preferred in the presence of the weak metal-atom interaction, however, they are in the presence of the strong metal-atom interaction. This effect is clearly a consequence of the lattice anisotropy and metal interaction strength chosen. In other words, the lattice induces an effective anisotropic interaction that can be difficult to control, and that has an effect on the morpho-

logies and effective connectivities of the clusters. This can be viewed as an artifact of the lattice if the intent is to model isotropic interactions, or it can be viewed as a simple way of observing the impact of anisotropy on the relationship between interaction strength and percolation.

VI. CONCLUSIONS

The present paper has attempted to address several issues associated with understanding the evolution of film growth resulting from metal-atom deposition onto a porous substrate. The simulation model has been developed in connection with experimental observations of the growth of a copper-polyimide interface and consequently a number of observed morphological features have paralleled what has been inferred from the model. Within this context the model has been useful in checking a number of conjectures prior to experiment and has captured some of the important elements of the physics responsible for the observation of certain interesting features and behavior.

The present paper focuses interest on a broad range of behavior inferred from the simulation model. This has been primarily motivated by an attempt to trace the evolution of film growth from the initial stages of deposition to the final stages of uniform film growth. Three different growth regimes have been identified: an initial low-deposition regime involving a distribution of small disconnected clusters, an intermediate regime encompassing the percolation threshold, and a high-deposition regime ultimately yielding continuous defect-free films. With regard to the percolation regime, previous models predicted conflicting results concerning shifts in the percolation threshold with thermal interactions. The present paper resolves these inconsistencies. Formal questions addressed in the present paper relating to percolation are the following. Should $(2+1)$-dimensional systems reveal different universal behavior from two- or three-dimensional systems? We have found that the model reveals two-dimensional universality. What role do length scales play with regard to connectivity and interactions for the annealed concentration of copper in a significant concentration gradient? We have found a crossover in the shift of the percolation transition which depends upon the interaction strength versus connectivity length. While the present paper has provided answers to these questions within the context of the on-site lattice model we have examined, other questions require further investigation, particularly with respect to diffusion mobility and the constraints imposed by the adoption of such a discrete lattice model.

Furthermore, even within the constraints of the present model, the complex and composite nature of this three-dimensional interfacial model provides a vast array of features of potential interest which we have presently not examined. The predominant intent of the present paper has been, therefore, to illustrate a certain number of these features and to raise questions associated with this particular type of interfacial growth rather than to provide a detailed set of definitive answers.

[1] B. D. Silverman, Macromolecules **24**, 2467 (1991).
[2] F. Faupel, D. Gupta, B. D. Silverman, and P. S. Ho, Appl. Phys. Lett. **55**, 357 (1989).
[3] R. F. Voss, R. B. Laibowitz, and E. I. Alessandrini, Phys Rev. Lett. **49**, 1441 (1982).
[4] A. Kapitulnik and G. Deutscher, Phys. Rev. Lett. **49**, 1982 (1982).
[5] A. L. R. Bug, S. A. Safran, G. S. Grest, and I. Webman, Phys. Rev. Lett. **55**, 1896 (1985).
[6] S. Hayward, D. W. Heerman, and K. J. Binder, Stat. Phys. **49**, 1053 (1987).
[7] E. V. Albano and H. G. Martin, Thin Solid Films, **151**, 121 (1987).
[8] T. DeSimone, R. M. Stratt, and S. Demoulini, Phys. Rev. Lett. **56**, 1140 (1986).
[9] M. Kolb, T. Gobron, J.-F. Gouyet, and B. Sapoval, Europhys. Lett. **11**, 601 (1990).
[10] F. K. LeGoues, B. D. Silverman, and P. S. Ho, J. Vac. Sci. Technol. A **6**, 2200 (1988).
[11] A. Foitzik and F. Faupel, Mat. Res. Soc. Symp. Proc. **203**, 59 (1990).
[12] N. Takahashi, D. Y. Yoon, and W. Parrish, Macromolecules **17**, 2583 (1984).
[13] B. J. Factor, T. P. Russell, and M. F. Toney, Phys. Rev. Lett. **66**, 1181 (1991).
[14] D. Stauffer, *Introduction to Percolation Theory* (Taylor and Francis, London, 1985).
[15] F. Family and T. J. Vicsek, J. Phys. A **18**, L75 (1985).
[16] P. Meakin and R. Julien, J. Phys. (Paris) **48**, 1651 (1987).
[17] R. P. Wool and J. M. Long, American Chemical Society Meeting, Washington, D.C., August 1990.
[18] S. Mazur and S. Reich, J. Phys. Chem. **90**, 1365 (1986).
[19] P. Meakin and R. Jullien, J. Phys. France **51**, 2673 (1990).
[20] R. F. Voss, J. Phys. A **17**, L373 (1984).
[21] B. Sapoval, M. Rosso, and J. F. Gouyet, J. Phys. Lett. **46**, L149 (1985).
[22] A. Z. Flammang, Phys. B **28**, 47 (1977).
[23] P. L. Leath, Phys. Rev. B **14**, 5046 (1976).

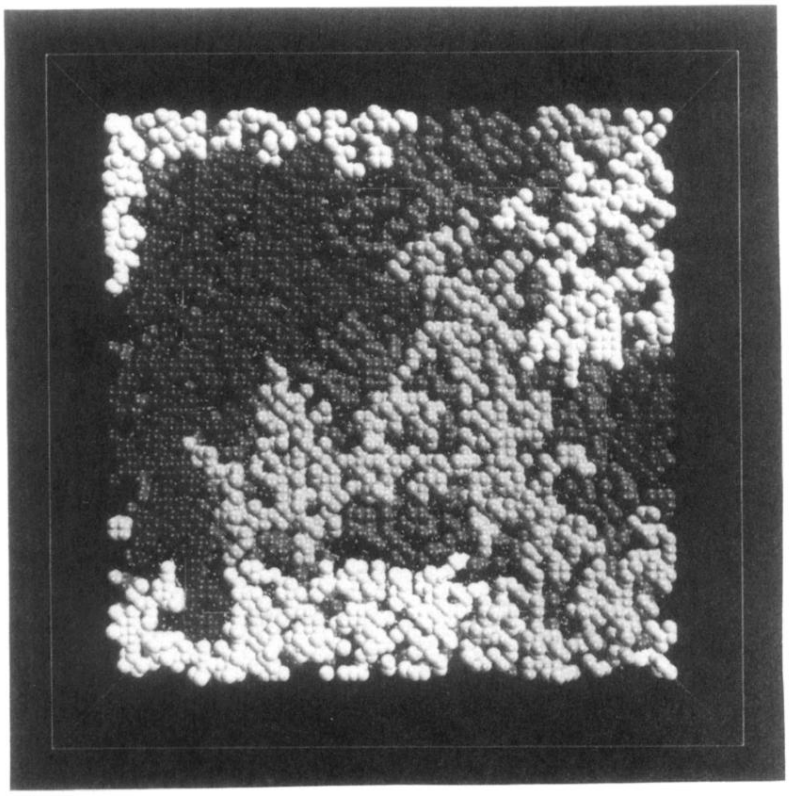

FIG. 13. Top view of a 0.72-monolayer deposition prior to annealing. Different grey scales indicate different clusters for far connectivity definition.

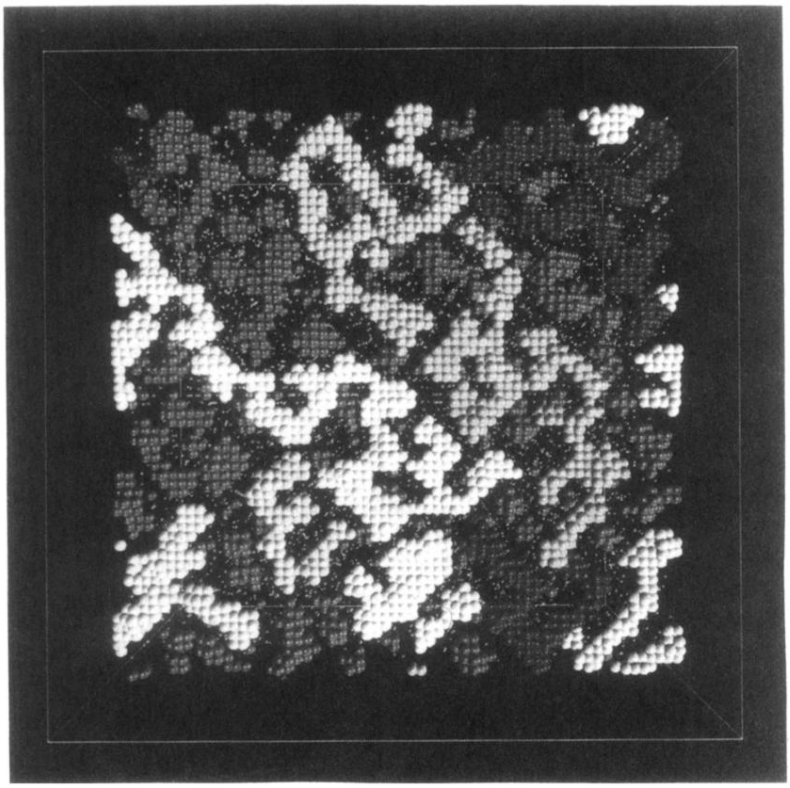

FIG. 14. Top view of a 1.1-monolayer deposition annealed at 320 °C. Different grey scales indicate different clusters for far connectivity definition. The metal-atom interaction is strong. Tiny spheres represent polymer interaction sites.